Solid Earth Discuss., 5, 2389–2418, 2013
www.solid-earth-discuss.net/5/2389/2013/
doi:10.5194/sed-5-2389-2013

Solid Earth
Discussions
Open Access

The sensitivity of GNSS measurements in Fennoscandia to distinct three-dimensional upper-mantle structures

H. Steffen[1] and P. Wu[2]

[1]Lantmäteriet, Lantmäterigatan 2c, 80182 Gävle, Sweden
[2]Department of Earth Sciences, The University of Hong Kong, Hong Kong, China

Received: 29 November 2013 – Accepted: 3 December 2013 – Published: 18 December 2013

Correspondence to: H. Steffen (holger-soren.steffen@lm.se)

Published by Copernicus Publications on behalf of the European Geosciences Union.

Abstract

We present the sensitivity of Global Navigation Satellite System (GNSS) measurements at selected GNSS stations used both in the EUREF Permanent Network as well as in the BIFROST project to distinct areas in a laterally heterogeneous upper mantle beneath Fennoscandia. We therefore use a three-dimensional finite element model for glacial isostatic adjustment (GIA) calculations. The underlying structure is based on the S20A seismic tomography model, whose shear-wave velocities have been transformed into a viscosity structure of the upper mantle. Lower mantle is not investigated as previous results showed negligible sensitivity of Fennoscandian GIA data to it. We subdivide the upper mantle in four layers with lateral viscosity structure. Areas with similar viscosity within a layer are combined to larger blocks. Further subdivision is made into areas inside and outside the formerly glaciated areas. This leads to about 20 differently shaped areas per layer. We then calculate the sensitivity kernels at 10 selected GNSS stations for all blocks in comparison to a well-fitting one-dimensional GIA model.

We find that GNSS stations are most sensitive to mantle viscosity in the near surrounding of the station, i.e. in the nearest about 250 km, and only within the formerly glaciated area. This area can be enlarged up to 800 km when velocities of stations in the uplift center are investigated. There is no indication of sufficiently high sensitivity of all investigated GNSS stations to regions outside the glaciated area. We also note that in the first mantle layer (70–250 km depth) below the lithosphere, there is only small sensitivity to parts along the Norwegian coast. Most prominent features in the Fennoscandian upper mantle may be detected in the second (250–450 km depth) and third layer (450–550 km depth).

In future investigations on the lateral viscosity structure using GNSS measurements one should only consider GNSS stations within the area of former glaciation. They can be further grouped to address certain areas. In a combination with other GIA data, e.g. relative sea-level and gravity data, it is then highly recommended to assign more

weight on those GNSS results with high sensitivity in order to determine the viscosity of a certain region.

1 Introduction

The process of glacial isostatic adjustment (GIA) allows the determination of Earth's structure, especially beneath formerly glaciated areas such as Fennoscandia and North America. The GIA process is indicated in and also affects multiple observations around the world. Here, relative sea-level data, Global Navigation Satellite System (GNSS) measurements and recently observations of the Gravity Recovery and Climate Experiment (GRACE) satellite mission are the most frequently employed ones in GIA investigations with dedicated models. They are used to identify model parameters such as lithospheric thickness and mantle viscosity. In recent years, owing to improved modelling techniques and advances in computation power, investigations regarding lateral variations of both lithospheric thickness and mantle viscosity were enabled. In view of that, it is important to understand the capability of the many GIA observations to determine these lateral variations. This study will analyze how sensitive class "A" GNSS stations of the EUREF Permanent Network (EPN, Bruyninx et al., 2013) are to distinct areas of similar viscosity in the upper mantle beneath Fennoscandia.

GIA observations such as mentioned above are equally sensitive to radial and lateral variations in mantle viscosity (Steffen et al., 2007). Sensitivity (or Fréchet) kernels of these GIA observations show how sensitive a quantity is to a specific region in the mantle, i.e. how much more or less sensitive it is compared to another region. Approaches to calculate sensitivity kernels were introduced by Mitrovica and Peltier (1991) and Peltier (1998) for a laterally homogeneous earth, and Wu (2006) if lateral heterogeneity is also allowed. For example, for the inversion of GIA observations, kernels were calculated for sensitivity of GIA observations to radial changes in viscosity (Mitrovica and Peltier, 1991, 1993, 1995; Peltier and Jiang, 1996a, b; Peltier, 1998). These studies showed that sensitivity is highest to the upper mantle, while sensitivity to the lower

SED
5, 2389–2418, 2013

mantle is much smaller. This is especially true for Fennoscandia, where the resolving power of GIA observations is too low to provide accurate results for lower-mantle viscosity at all (Mitrovica and Peltier, 1993; Steffen and Wu, 2011). In North America though, more information about the lower mantle can be retrieved because of the higher sensitivities to at least the shallow lower mantle (Mitrovica and Peltier, 1995).

Milne et al. (2004) presented with the help of a one-dimensional (1-D) model kernels for the velocity field at selected Fennoscandian GNSS stations of the BIFROST (Baseline Inferences for Fennoscandian Rebound Observations, Sea Level, and Tectonics) project to radial viscosity. Interestingly, they found sufficiently high sensitivities for the lower mantle when compared to sensitivities for the upper mantle. This was not supported by Steffen et al. (2006), who showed with a three-dimensional (3-D) model that lateral variations in lower-mantle viscosity do not affect the GNSS velocity field in Fennoscandia. As pointed out in Wu (2006), the sensitivity of the Fennoscandian data to the lower mantle may actually be due to contribution from Laurentia!

Sensitivity to lateral viscosity variations were further investigated by Wu (2006) and Steffen et al. (2007). While Wu (2006) presented a global investigation with an axisymmetric (two-dimensional) model and simplistic ice load, Steffen et al. (2007) focused on the GNSS stations in Fennoscandia as used by Milne et al. (2004) with a 3-D model and realistic (four-dimensional) ice load. The advantage of the model used by Steffen et al. (2007) compared to Wu (2006) was that all components of the velocity field could be analyzed in conjunction with a realistic ice load. Steffen et al. (2007) investigated the sensitivity of blocks with 600 km × 600 km or 1000 km × 1000 km size, which are equally distributed blocks within the model. Both studies showed that sensitivity is highest within the former glaciated area to about 450–550 km depth. The distribution and deglaciation history of the ice strongly affect the magnitude of sensitivity (Steffen et al., 2007). If one is interested in a certain area outside the former glaciated area, one should analyze horizontal velocities. In this regards, Steffen et al. (2007) additionally noted that this depends on the size of the perturbed mantle region. They suggested further investigation with a more realistic viscosity structure in the mantle.

SED
5, 2389–2418, 2013

This study will investigate such a viscosity structure. We therefore use a commonly used GIA model with a lateral viscosity distribution in the upper mantle, which has been used in former studies, as well as a realistic ice sheet. We then determine the sensitivity of selected GNSS stations to distinct regions of similar viscosity in the upper mantle beneath Fennoscandia. The GNSS stations used in this study (Fig. 1) belong to the best and well-maintained stations of the EPN. They are considered as class "A" stations, thus their positions have an accuracy of 1 cm at all epochs of the time span of the used observations (Bruyninx et al., 2013). One exception is the station Vaasa, which is of class "B" (positions with an accuracy of 1 cm at the epoch of minimal variance of the station). The selected stations are also used in BIFROST investigations to GIA (see Lidberg et al., 2010).

The aims of this study are (i) to identify and categorize the sensitivity of the stations (i.e. the velocity field determined there) to a viscosity block depending on the location of the station and the block – and here also in view of their location to the former ice sheet – and (ii) outline where future GNSS stations in Fennoscandia would be helpful to identify lateral viscosity changes. The next section describes the model used, followed by the presentation and discussion of the results. We finally conclude in Sect. 5.

2 Modelling

The GIA process in Fennoscandia is modelled with a flat, layered, isotropic, compressible, Maxwell-viscoelastic, laterally heterogeneous finite-element model as described in Steffen et al. (2006). Such models based on an approach by Wu (2004) have been successfully used in many GIA investigations regarding North America (e.g. Wu, 2005), Fennoscandia (e.g. Steffen et al., 2006), the Barents Sea (e.g. Kaufmann and Wu, 1998), Antarctica (e.g. Kaufmann et al., 2005) and Iceland (e.g. Schmidt et al., 2012). It consists of a central area of 3000 km × 3000 km size, where each element has a horizontal side length of 100 km. The ice-load history from the regional ice model FBKS8 (Lambeck et al., 1998) is applied to the surface in the central area. Outside the central area is a peripheral frame of 60 000 km width to allow the mantle material to flow due to application of a surface load outside the area of interest.

We use two models from Steffen et al. (2006) and keep their naming. Model U3L1_V1 has a uniform 70 km thick lithosphere on top, followed by four layers of the upper mantle and another four of the lower mantle. The upper mantle has laterally varying viscosities in each layer, which are converted from the seismic shear-wave tomography model S20A (Ekström and Dziewonski, 1998). The viscosity structure within the four upper-mantle layers is shown in Fig. 2 with solid black lines. Model U1L1_V1 is the same as U3L1_V1, but has no laterally varying viscosity in the upper mantle. Here, a value of 4×10^{20} Pa s is assigned, which represents a good average of upper-mantle viscosity in Fennoscandia (Steffen and Wu, 2011). Lower-mantle viscosity in both models is set to 2×10^{22} Pa s. Each element within a layer is assigned volume-averaged values of density ρ, shear modulus μ and bulk modulus κ as derived from the Preliminary Reference Earth Model (PREM Dziewonski and Anderson, 1981). An overview of the depths and values of the material parameters of each layer is provided in Table 1 of Steffen et al. (2006).

Sensitivity is investigated for certain blocks within a layer. To do this, the viscosity structure within a layer is grouped into blocks of similar viscosity, see red lines in Fig. 2. These blocks of similar viscosity are further subdivided in blocks that lie inside the former glaciated area and those lying outside. With this subdivision of the mantle layers we can investigate the sensitivity behavior of a block as a relation of its location to the former ice sheet. In addition, we design three blocks in the center of uplift, which have the same shape in all four layers. With this subdivision we overcome the different shapes of the blocks between the layers and are able to investigate sensitivity kernels as a function of depth. The total number of blocks is 78. In the first upper-mantle layer there is the maximum number of blocks with 22. The lowest number of blocks is with 18 in the third layer. The other two layers have 19 blocks each. Numbering starts with the three central blocks and then continues counterclockwise from the North, first inside, then outside the former glaciated area. The subdivision in terms of similar viscosity is

SED
5, 2389–2418, 2013

in one order of magnitude steps in the first layer. In the other three layers it is every half order of magnitude. The subdivision does not always follow exactly the isolines of viscosity nor the extent of the ice sheet. This is not of major importance as we employ two models (ice and seismic tomography model) only as examples in a test. Other models, e.g. the ice-load history of ICE-5G (Peltier, 2004) or the seismic tomography model by Grand et al. (1997), will prefer other subdivisions. But, we will show that the results from our investigation will most likely hold also for other (ice and tomography) models.

3 Results

We calculate normalized sensitivity kernels $K_{lj}(r_i)$ of block j in layer i at location l following an approach introduced by Peltier (1998) and slightly modified by Wu (2006):

$$K_{lj}(r_i) = \frac{\delta p_l}{\delta m_j(r_i)\,\Delta V_j(r_i)\,V_{\max}(r_i)}, \tag{1}$$

with δp_l the differential prediction between the prediction p_l^{3-D} of a certain perturbed 3-D model and the prediction p_l^{1-D} of the U1L1_V1 model at location l, $\delta m_j(r_i)$ the viscosity perturbation of block j in layer i and $\Delta V_j(r_i)$ the fractional volume of this particular block. The latter

$$\Delta V_j(r_i) = \frac{V_j(r_i)}{V_{\text{model}}}, \tag{2}$$

with $V_j(r_i)$ the block volume, and V_{model} the volume of the entire central area in the model, which includes the upper and lower mantle. $V_{\max}(r_i)$ is the maximum fractional volume of each layer, i.e. the largest block volume in a layer, which is used to normalize the kernel. This normalization is possible as the relative amplitude is important for the sensitivity kernels rather than their absolute amplitude. Thus, we do not provide

SED
5, 2389–2418, 2013

absolute values which can be compared to the accuracies of GNSS observations, but we show to which areas a station is most sensitive. $V_1(r_2)$, for example, refers to the volume of block 1 in the second layer shown in Fig. 2. A prediction p_l is one of the velocities. The viscosity perturbation is set as magnitude difference between the viscosity of the block in model U3L1_V1 and the upper-mantle viscosity in model U1L1_V1 (4×10^{20} Pa s).

The kernels for each velocity are calculated for the location of each of the 10 selected EPN stations. Thus, we are able to analyze the relative sensitivity of the station to every block.

Figure 3 presents exemplarily, for the two stations Kiruna and Brussels, the sensitivity kernels for three velocity components (EW, NS, Z) to all the different viscosity blocks in the model. Kiruna (Fig. 3a) is located above block 1 in each layer and also not too far away from the former area of maximum glaciation. It is apparent that sensitivity of any velocity component to a block in the first mantle layer (70–250 km depth) is almost negligible. The plot also shows that sensitivity is highest to blocks right underneath the station or in the near surrounding, but generally within the area of former glaciation. The largest sensitivity in the vertical velocity is found to block 1 in the second mantle layer (250–450 km depth). This is also the highest sensitivity found for any velocity at one of the 10 selected stations to any block. In the same layer, sensitivity is also relatively large to the two neighboring blocks in the north (block 4) and south (block 2). For all other blocks in this layer the sensitivity is much smaller. Sensitivity of the vertical component is also eye-catching in blocks 1, 2 and 5 of the third mantle layer (450–550 km depth) as well as blocks 1 and 4 in the fourth mantle layer (550–670 km depth). Horizontal velocity sensitivities are generally smaller. However, their horizontal extent is the largest in the second layer, and their amplitude decreases with depth.

For the station of Brussels (Fig. 3b), which is located outside the former area of glaciation, sensitivities of all velocities to any block in any layer are almost negligible. This also holds for the viscosity blocks underneath the station. Any sensitivity that is

SED
5, 2389–2418, 2013

marginally indicated is related to horizontal velocities and located within the area of former glaciation.

The representation of kernels as in Fig. 3 can be repeated for the other stations as well. However, this illustration may not be helpful in clearly identifying the blocks (and thus areas) of major or significant sensitivity in the velocities. To overcome this, we set a threshold sensitivity. As the sensitivities presented are normalized and thus a relative measure, we may choose an arbitrary value within the range indicated in the ordinate of Fig. 3. From the 10 stations, Kiruna shows the largest kernel values, while Brussels has the lowest. After testing, we find a threshold of 0.05 $\mathrm{mm\,yr^{-1}}$, which provides helpful insights in the sensitivity of the vertical velocity. This value corresponds to about 0.5 % of the maximum uplift velocity of about 1 $\mathrm{cm\,yr^{-1}}$ observed in Fennoscandia. A threshold of 0.015 $\mathrm{mm\,yr^{-1}}$ is found to be reasonable for the horizontal velocities. Figures 4–12 provide an overview of the blocks to which the velocities observed at 9 of the stations are sensitive to. Velocities at the Brussels GNSS station are not sensitive to any viscosity block when the selected thresholds are applied, and thus we do not show a figure here. Please note that we mean sensitivity above the selected threshold of a velocity to a certain block in the following discussion when we write about sensitivity.

GNSS-derived velocities at Kiruna (Fig. 4) are sensitive to several blocks in a layer. However, not all components of the velocity field are always sensitive to the same viscosity block. In the first mantle layer, horizontal velocities show a sensitivity to blocks in the west of the station at the edge of the former ice sheet. Vertical velocity is insensitive here to any viscosity block. In the second mantle layer, however, sensitivity arises to the block below the station as well as to the block north and south of it. In addition, a block in the southwest is detectable by vertical velocity. Horizontal velocities may provide information for the underlying block, the EW component also for blocks in the west and east of this block, the NS component for the ones in the north and south of it. In the third layer there are less viscosity blocks than in the second layer which have high enough sensitivity in the velocity field. The vertical component is sensitive to the underlying block and blocks south and west of it, the EW component to the block

SED
5, 2389–2418, 2013

west of the station, the NS component to block 3 about 400 km south of the station. In the lowermost upper-mantle layer only the underlying block influences the vertical component. Three blocks lead to sensitivity in the horizontal components; the block in the west in the EW component, the block in the north in NS component, and a block further in the south in the NS component as well.

The stations of Skellefteå (Fig. 5), Vaasa (Fig. 6) and Mårtsbo (Fig. 7) show similar patterns like Kiruna. Interestingly, there is sensitivity of the vertical component in Skellefteå to a block east of the station mainly outside the former glaciated area in the third layer. There is also sensitivity of the vertical component in Vaasa to the underlying block in the first layer.

The sensitivity pattern changes for the stations of Oslo (Fig. 8) and Onsala (Fig. 9). There is a clear dominance of sensitivities to nearby blocks in the second mantle layer, while blocks especially in the first and third layer yield mostly no significant sensitivities. In the case of Onsala, no sensitivity is observed to the third layer at all. At Smidstrup (Fig. 10), eventually, only sensitivities by the vertical component to two blocks of the second mantle layer are found.

At Svetloe (Fig. 11) the pattern is different compared to the other stations. Only similarity is that the second mantle layer is the layer with the most blocks that show sufficient sensitivity in the velocities. In the other three layers, horizontal velocities, and here especially the EW component, highlight a sensitivity to blocks located underneath the central Norwegian coast. This also holds partly for the second layer. There are also blocks near the center of former glaciation which yield larger sensitivities than the threshold. In Riga (Fig. 12), which is a station further southwest from Svetloe, but still within the former glaciated area, the number of blocks with sensitivity above the threshold is much lower. However it is not sensitive to the viscosity structure directly below, also here a sensitivity of the horizontal velocities to the area of the Norwegian coast is indicated in the third layer, as well as the sensitivity to the block in the southern center of the Scandinavian Peninsula in the second layer. In the first and fourth layer sensitivity of all blocks lies below the threshold.

SED
5, 2389–2418, 2013

4 Discussion

It becomes evident that sufficient sensitivity mainly yields for viscosity blocks that are located inside the former glaciated area. This sensitivity affects all velocity components, with the strongest influence in the vertical component. However, the sensitivity will most likely be only large enough for GNSS stations that are located inside the former glaciated area as well. The maximum sensitivity results in the center with maximum glaciation. Not only large sensitivities are observed in all components here, also blocks in all layers show large sensitivities.

The central stations of Kiruna, Skellefteå, Vaasa and Mårtsbo are sensitive to the area along the Norwegian Atlantic coast, that has both strong gradients in viscosity in the first layer and is located near the edge of glaciation. The stations of Oslo, Onsala and Svetloe are sensitive to a certain block (number 8 in UM1 in Fig. 2) in this area as well. The strong gradient is due to the fixed lithospheric thickness of 70 km in the model, but it is well known that there is a strong lateral variation, i.e. a thickening from west to east, in Fennoscandia (Steffen and Wu, 2011). This is simulated with higher and thus stiffer viscosities in the first mantle layer. Thus, sensitivity to viscosity blocks in the first mantle layer also implies sensitivity to lithospheric thickness variations.

All three velocity components observed at the GNSS stations in the center of glaciation or in the southern part of the Scandinavian Peninsula are sensitive to the underlying block in the second layer. Here, the maximum sensitivities for a particular station are usually found. Sensitivities larger than the threshold are also determined for the surrounding blocks, which are generally nearby blocks for the vertical component. In the horizontal components, blocks located in the north or south of the station show sensitivity in the NS component, while blocks in the east or west of the station reflect sensitivity in the EW component. The two stations in the immediate center of glaciation, Skellefteå and Vaasa highlight the most blocks in the second layer. Both stations are with at least one velocity component sensitive to almost every (only one is missing) viscosity block within the former glaciated area. The number of blocks in the second layer that stations show enough sensitivity to, is reduced as the station moves away from the glaciation center. Also, these blocks are generally located in the vicinity of the GNSS station, i.e. within a radius of about 500 km.

Of interest is block number 7 in the second layer (Fig. 2) in the southern center of the Scandinavian Peninsula. All stations within the former glaciated area show a sensitivity of at least one velocity component to this particular block. This may mean that in GIA inversions for mantle viscosity with a majority of GNSS stations within the former glaciated area (and assuming that our used viscosity structure as derived from model S20A as well as the ice model represent reality without a doubt), the determined viscosity of a larger area value is strongly referring to this particular area only. Also, by comparing the viscosity inferred from the vertical component of GNSS stations within the former glaciated area and the one inferred without the ones in the center, one should get hints on the accurate viscosity of this area.

Sensitivity of the velocity components to the third mantle layer (450–550 km depth) is smaller than that for the second layer (250–450 km depth). Velocities at three stations (Onsala and Smidstrup in addition to Brussels) are not sensitive to any block at all. Onsala and Smidstrup are located within about 300 km distance to the glaciation limit and thus far away from the glaciation maximum. The stations of Oslo, Riga and Svetloe in mid-distance have small sensitivities to one block only. While for Oslo the vertical component is sensitive to the underlying block, the other two stations have one of the horizontal components sensitive to the Norwegian coast area, which is on the opposite side of the glaciated area. Here, the chosen threshold value may lead to this pattern. It appears that it is close to the sensitivity values in all three velocity components of mid-distance GNSS stations. Hence, future investigations should address if these stations can deliver enough information of the third layer in an absolute manner when taking the accuracy of GNSS measurements into account.

The stations closer to the center and thus larger ice thickness show comparable pattern as for the second layer, but with a smaller range of blocks in the surrounding of the GNSS station they are sensitive to. The distance is 600 km at most. An exception is block number 17 (Fig. 5, UM3), which is mainly located outside the former glaciated area. Here, the vertical component in Skellefteå is sensitive to it. As no other block shows a high sensitivity above the threshold in any of the stations (including Skellefteå), it may be an accidental case.

The fourth mantle layer cannot be investigated with GNSS data from Smidstrup and Riga. The stations of Onsala and Svetloe indicate sensitivity to the Norwegian coast area again. Oslo instead may give insight into two blocks underneath the station. The stations located closer to or in the center mainly repeat the pattern of the second layer, but show a lower number of blocks they are sensitive to. However, these stations cover blocks within a range of up to 800 km, and thus should provide useful information of the lowest part of the upper mantle underneath the Scandinavian Peninsula.

Our results strongly support the usage of stations in the center such as Skellefteå or Vaasa for investigations on the viscosity structure in the upper mantle. The vertical component is giving information of the viscosity structure in an area of 500 to 800 km around the station from about 250 to 670 km depth. Horizontal velocities may enlarge this area to more than 1000 km, especially in the second and fourth layer. The further one goes away from the center, the less information can be obtained. The interesting result here is that the area around the Norwegian coast is a dominating signal in the horizontal velocity component of many GNSS stations also on the other side of the former glaciated area, e.g. in Riga and Svetloe. A thorough analysis of a set of horizontal velocities in this area can probably result in viscosity estimates referring to this respective area. Moreover, it is the only area where horizontal components are found to be sensitive to each layer in the upper mantle. Stations outside the former glaciated area cannot be used.

Oceanic areas far off the coast, i.e. the ones that were also never affected by ice load on top, do not show any significant sensitivity at any GNSS station. We further note that blocks in the southwest imply insignificant sensitivities. This may be different if ice load on the British Isles is investigated. Future investigations with British GNSS stations should analyze their potential sensitivity for the area.

SED
5, 2389–2418, 2013

H. Steffen and P. Wu

5 Conclusions

We presented the sensitivity of 10 selected GNSS stations to a realistic structure of lateral viscosity variations under Fennoscandia. The GNSS stations are backbones of the EPN and the BIFROST project and thus represent excellent and well-maintained stations of high accuracy. We employed a 3-D finite element model that has been commonly used in the last two decades. A realistic ice load of the ice model FBKS8 (Lambeck et al., 1998) was applied.

Our results confirm that GNSS stations are most sensitive to viscosity changes underneath a station (see e.g. Milne et al., 2004; Steffen et al., 2007), but mainly in a depth below 250 km. This has been found by Steffen et al. (2007) as well. Both horizontal and vertical velocities show significant sensitivities. However, we further note that this only holds for GNSS stations located within the area of former glaciation, and here especially to stations in the uplift center. The depth of sensitivity goes parallel with ice thickness, the less ice the less information can obtained from the fourth layer, which confirms the resolving power of GIA data in general.

The sensitivity is mainly limited to the viscosity blocks right underneath (thus to a lateral extent of about 250 km) and also to a few other blocks nearby if these blocks or parts of such a block are located within a lateral distance of about 500 km to 800 km and if the station is located in the uplift center or in mid-distance to it. This is in contrast to the findings by Steffen et al. (2007), who showed that the sensitivity of neighboring blocks is mainly negligible. This difference is related to the regular block structure used in Steffen et al. (2007). Thus, it is important for future studies to investigate the sensitivity of our conclusions with a different block structure, which is based, for example, on a different seismic tomography model.

Stations outside the former glaciated area do not highlight sufficient sensitivity to viscosity underneath. This is different to the findings by Steffen et al. (2007), who found a slight indication that such horizontal velocities of such stations might be helpful. This is probably due to the approach of averaging the kernels of a block they used. This may

SED
5, 2389–2418, 2013

have increased the kernel value for blocks that covered glaciated and non-glaciated areas. It should be noted that Steffen et al. (2007) already suggested to use a more realistic viscosity block structure for a sophisticated analysis to find out if their result is correct or not.

Regarding planning of future GNSS stations for GIA research and additionally the question: which existing stations should be considered for GIA investigations, e.g. within the BIFROST project, it becomes evident that mainly stations within the former glaciated area should be considered. There is a dense network installed in the countries of Norway, Sweden, Finland and Denmark, which will be further densified in the next years. In Sweden, for example, the network will consist of 400 stations by 2020 (Lantmäteriet, 2011). Recently, 20 stations of the existing network have been proposed as new EPN stations (Engberg et al., 2013), which demonstrates the quality of the observed data. Thus, an adequate network of GNSS stations already exists which allows thorough investigations. Wu et al. (2010) investigated optimal locations for GNSS stations in Fennoscandia. In view of lateral viscosity variations (and also other GIA modelling parameters), they suggested more stations in the Baltic States and NW Russia. Our results clearly support this argument as both regions are located within the former glaciated area.

The results from this study are helpful in future investigations on lateral variations of mantle viscosity and lithospheric thickness. We recommend a careful grouping of GNSS velocity fields from selected areas, e.g. from the uplift center or the Baltic States, to investigate the vertical viscosity profile underneath the uplift center or the viscosity structure of the Norwegian coast, respectively. In combined analyses with other GIA observations such as relative sea-level data or gravity on ground and in space we highly recommend to assign more weight to a specific regional GNSS result when focusing on one of the regions in Fennoscandia discussed in our study.

Acknowledgements. We thank Kurt Lambeck for providing the FBKS8 ice model. Figures are prepared using GMT software (Wessel and Smith, 1998).

References

Bruyninx, C., Altamimi, Z., Caporali, A., Kenyeres, A., Lidberg, M., Stangl, G., and Torres, J. A.: Guidelines for EUREF densifications, IAG sub-commission for the European Reference Frame – EUREF, available at: ftp://epncb.oma.be/pub/general/Guidelines_for_EUREF_Densifi_cations.pdf, 2013. 2391, 2393

Dziewonski, A. M. and Anderson, D. L.: Preliminary reference Earth model, Phys. Earth Planet. In., 25, 297–356, doi:10.1016/0031-9201(81)90046-7, 1981. 2394

Ekström, G. and Dziewonski, A. M.: The unique anisotropy of the Pacific upper mantle, Nature, 394, 168–172, doi:10.1038/28148, 1998. 2394, 2408

Engberg, L. E., Engfeldt, A., Jivall, L., Kempe, C., Lidberg, M., Lilje, C., Lilje, M., Norin, D., Steffen, H., Wiklund, P., and Ågren, J.: National Report of Sweden to the EUREF 2013 Symposium – activities at Lantmäteriet, Report, 8 pp., available at: http://euref2013.fomi.hu/Download/Session_6/Sweden_NationalReport2013_paper.pdf, 2013. 2403

Grand, S. P., Van Der Hilst, R. D., and Widiyantoro, S.: Global seismic tomography: a snapshot of convection in the earth, GSA Today, 7, 1–7, 1997. 2395

Kaufmann, G. and Wu, P.: Lateral asthenospheric viscosity variations and postglacial rebound: a case study for the Barents Sea, Geophys. Res. Lett., 25, 1963–1966, doi:10.1029/98GL51505, 1998. 2393

Kaufmann, G., Wu, P. and Ivins, E. R.: Lateral viscosity variations beneath Antarctica and their implications on regional rebound motions and seismotectonics, J. Geodyn., 39, 165–181, doi:10.1016/j.jog.2004.08.009, 2005. 2393

Lambeck, K., Smither, C., and Johnston, P.: Sea-level change, glacial rebound and mantle viscosity for northern Europe, Geophys. J. Int., 134, 102–144, doi:10.1046/j.1365-246x.1998.00541.x, 1998. 2393, 2402, 2408

Lantmäteriet: Geodesy 2010 – a strategic plan for Lantmäteriet's geodetic activities 2011–2020, Lantmäteriet, Gävle, Sweden, available at: http://www.lantmateriet.se/upload/filer/kartor/geodesi_gps_och_detaljmatning/geodesi/Geodesy_2010.pdf, 2011. 2403

Lidberg, M., Johansson, J. M., Scherneck, H.-G., and Milne, G. A.: Recent results based on continuous GPS observations of the GIA process in Fennoscandia from BIFROST, J. Geodyn., 50, 8–18, doi:10.1016/j.jog.2009.11.010, 2010. 2393

Milne, G. A., Mitrovica, J. X., Scherneck, H.-G., Davis, J. L., Johansson, J. M., Koivula, H., and Vermeer, M.: Continuous GPS measurements of postglacial adjustment in Fennoscan-

dia: 2. Modeling results, J. Geophys. Res., 109, B02412, doi:10.1029/2003JB002619, 2004. 2392, 2402
Mitrovica, J. X. and Peltier, W. R.: A complete formalism for the inversion of post glacial rebound data: resolving power analysis, Geophys. J. Int., 104, 267–288, doi:10.1111/j.1365-246X.1991.tb02511.x, 1991. 2391
Mitrovica, J. X. and Peltier, W. R.: The inference of mantle viscosity from an inversion of the fennoscandian relaxation spectrum, Geophys. J. Int., 114, 45–62, doi:10.1111/j.1365-246X.1993.tb01465.x, 1993. 2391, 2392
Mitrovica, J. X. and Peltier, W. R.: Constraints on mantle viscosity based upon the inversion of post-glacial uplift data from the Hudson Bay region, Geophys. J. Int., 122, 353–376, doi:10.1111/j.1365-246X.1995.tb07002.x, 1995. 2391, 2392
Peltier, W. R.: The inverse problem for mantle viscosity, Inverse Probl., 14, 441–478, doi:10.1088/0266-5611/14/3/006, 1998. 2391, 2395
Peltier, W. R.: Global glacial isostasy and the surface of the iceage earth: the ICE-5G (VM2) model and GRACE, Annu. Rev. Earth Pl. Sc., 32, 111–149, doi:10.1146/annurev.earth.32.082503.144359, 2004. 2395
Peltier, W. R. and Jiang, X.: Glacial isostatic adjustment and earth rotation: refined constraints on the viscosity of the deepest mantle, J. Geophys. Res., 101, 3269–3290, doi:10.1029/95JB01963, 1996a. 2391
Peltier, W. R. and Jiang, X.: Mantle viscosity from the simultaneous inversion of multiple data sets pertaining to postglacial rebound, Geophys. Res. Lett., 23, 503–506, doi:10.1029/96GL00512, 1996b. 2391
Schmidt, P., Lund, B., Árnadóttir, T., and Schmeling, H.: Glacial isostatic adjustment constrains dehydration stiffening beneath Iceland, Earth Planet. Sc. Lett., 359–360, 152–161, doi:10.1016/j.epsl.2012.10.015, 2012. 2393
Steffen, H. and Wu, P.: Glacial isostatic adjustment in Fennoscandia – a review of data and modeling, J. Geodyn., 52, 169–204, doi:10.1016/j.jog.2011.03.002, 2011. 2392, 2394, 2399
Steffen, H., Kaufmann, G., and Wu, P.: Three-dimensional finite-element modelling of the glacial isostatic adjustment in Fennoscandia, Earth Planet. Sc. Lett., 250, 358–375, doi:10.1016/j.epsl.2006.08.003, 2006. 2392, 2393, 2394
Steffen, H., Wu, P., and Kaufmann, G.: Sensitivity of crustal velocities in Fennoscandia to radial and lateral viscosity variations in the mantle, Earth Planet. Sc. Lett., 257, 474–485, doi:10.1016/j.epsl.2007.03.002, 2007. 2391, 2392, 2402, 2403

Wessel, P. and Smith, W. H. F.: New, improved version of generic mapping tools released, EOS, 79, 579, doi:10.1029/98EO00426, 1998. 2403

Wu, P.: Using commercial finite element packages for the study of earth deformations, sea levels and the state of stress, Geophys. J. Int., 158, 401–408, doi:10.1111/j.1365-246X.2004.02338.x, 2004. 2393

Wu, P.: Effects of lateral variations in lithospheric thickness and mantle viscosity on glacially induced surface motion in Laurentia, Earth Planet. Sc. Lett., 235, 549–563, doi:10.1016/j.epsl.2005.04.038, 2005. 2393

Wu, P.: Sensitivity of relative sea levels and crustal velocities in Laurentide to radial and lateral viscosity variations in the mantle, Geophys. J. Int., 165, 401–413, doi:10.1111/j.1365-246X.2006.02960.x, 2006. 2391, 2392, 2395

Wu, P., Steffen, H., and Wang, H. S.: Optimal locations for GPS measurements in North America and northern Europe for constraining glacial isostatic adjustment, Geophys. J. Int., 181, 653–664, doi:10.1111/j.1365-246X.2010.04545.x, 2010. 2403

SED

5, 2389–2418, 2013

Sensitivity of GNSS stations to 3-D upper-mantle viscosity

H. Steffen and P. Wu

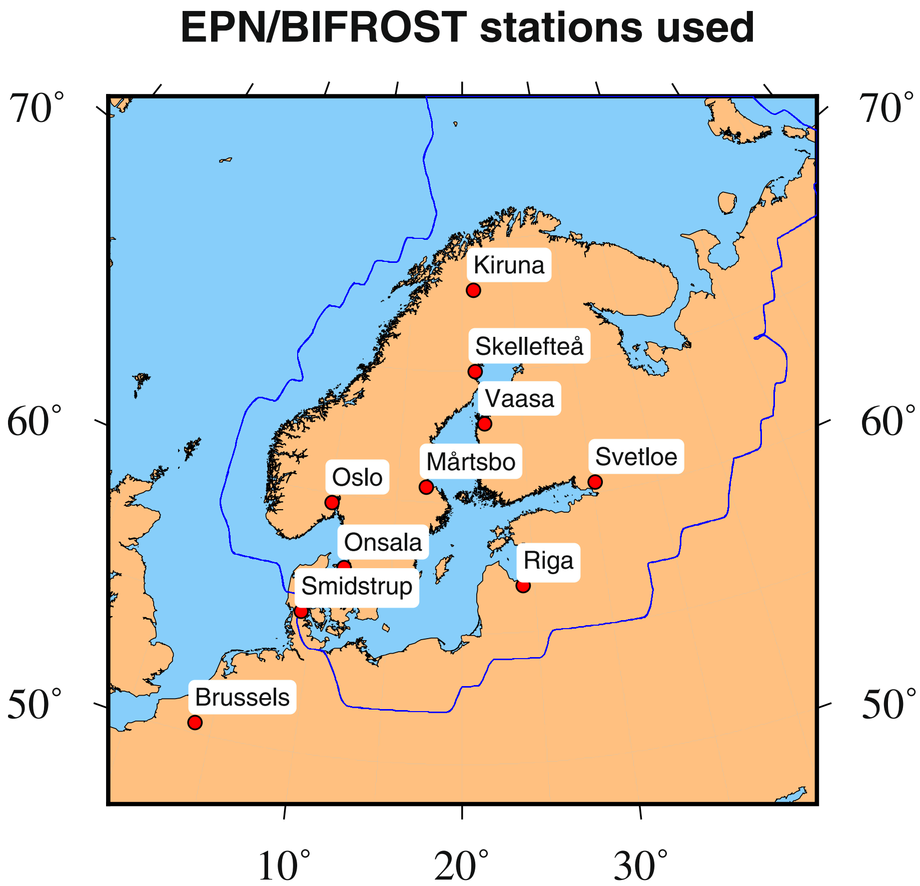

Fig. 1. Overview of EPN/BIFROST station used in our investigation.

SED
5, 2389–2418, 2013

Sensitivity of GNSS stations to 3-D upper-mantle viscosity

H. Steffen and P. Wu

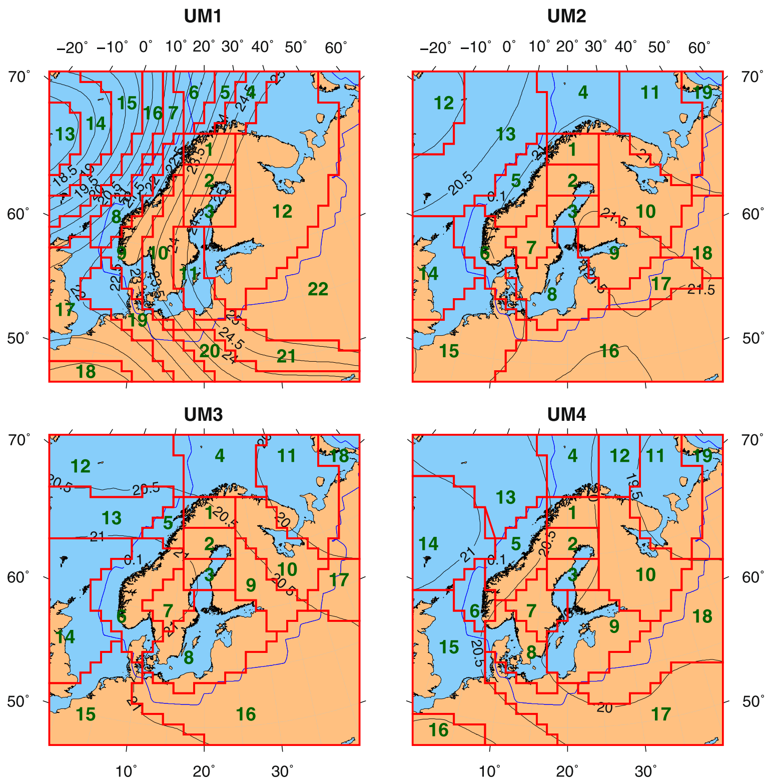

Fig. 2. Distribution of viscosity blocks (red lines, green numbers) based on the lateral viscosity structure (black lines) as calculated from seismic tomography model S20A (Ekström and Dziewonski, 1998). Viscosity blocks are additionally subdivided into blocks inside and outside the former glaciated area (blue line, based on ice model FBKS8; Lambeck et al., 1998). Depth ranges: UM1 70–250 km, UM2 250–450 km, UM3 450–550 km, UM4 550–670 km.

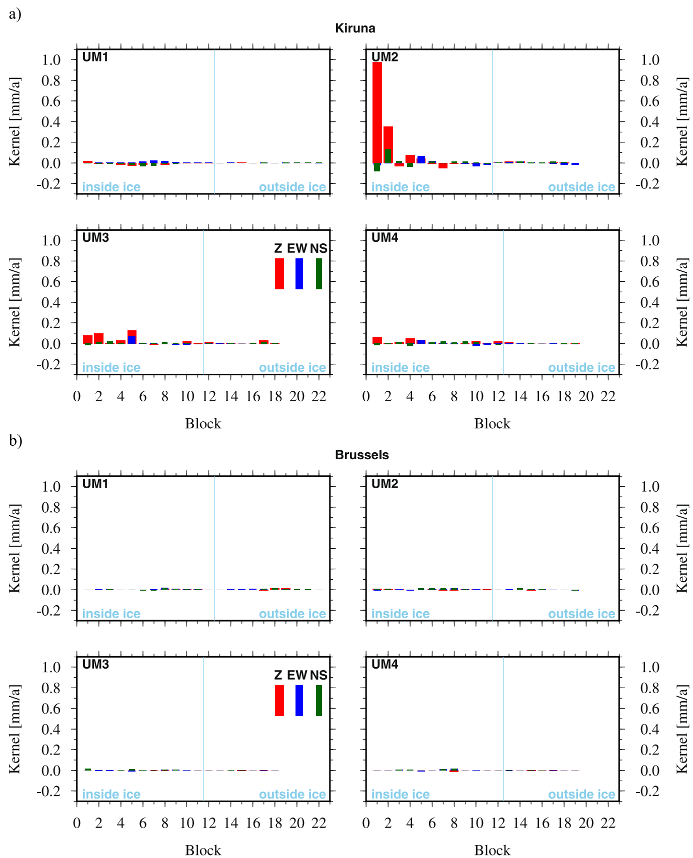

Fig. 3. Sensitivity kernels shown as bars for vertical (red) and horizontal velocities (EW: blue, NS: green) at the stations of **(a)** Kiruna, and **(b)** Brussels to viscosity blocks in the four layers of the upper mantle (UM1–UM4). Depth ranges: UM1 70–250 km, UM2 250–450 km, UM3 450–550 km, UM4 550–670 km.

SED
5, 2389–2418, 2013

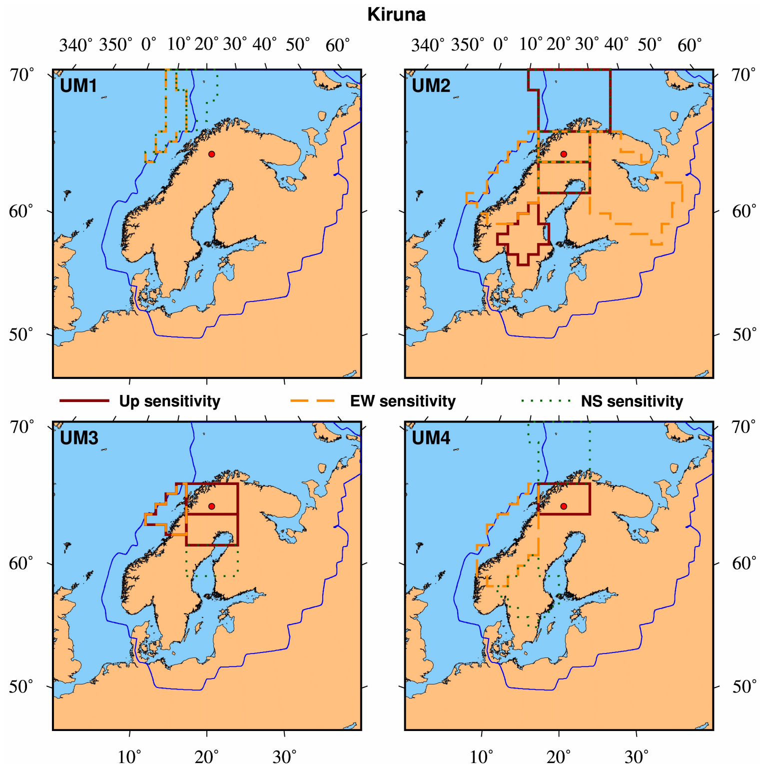

Fig. 4. Location of viscosity blocks in each layer where sensitivity kernels of the velocities in Kiruna (red dot) lie above selected threshold. Red solid line: vertical velocity. Orange dashed line: EW velocity. Green dotted line: NS velocity. Blue line: former glaciated area based on ice model FBKS8. Depth ranges: UM1 70–250 km, UM2 250–450 km, UM3 450–550 km, UM4 550–670 km.

SED
5, 2389–2418, 2013

Sensitivity of GNSS stations to 3-D upper-mantle viscosity

H. Steffen and P. Wu

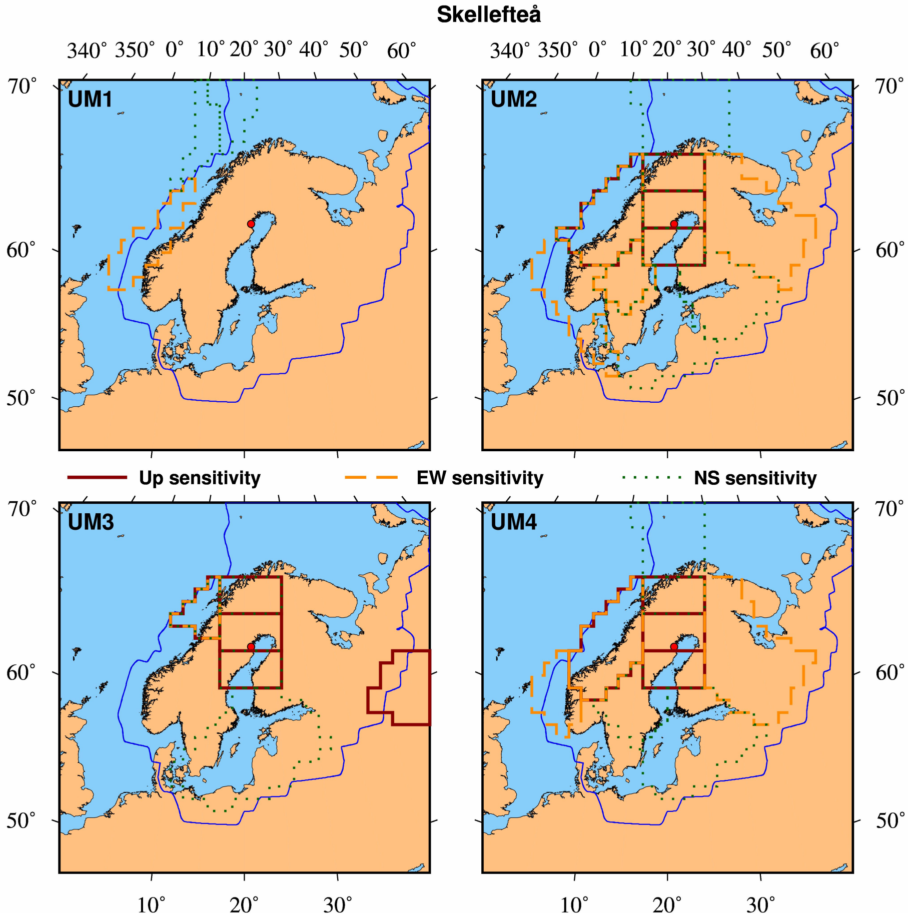

Fig. 5. Same as Fig. 4, but for Skellefteå.

SED
5, 2389–2418, 2013

Sensitivity of GNSS stations to 3-D upper-mantle viscosity

H. Steffen and P. Wu

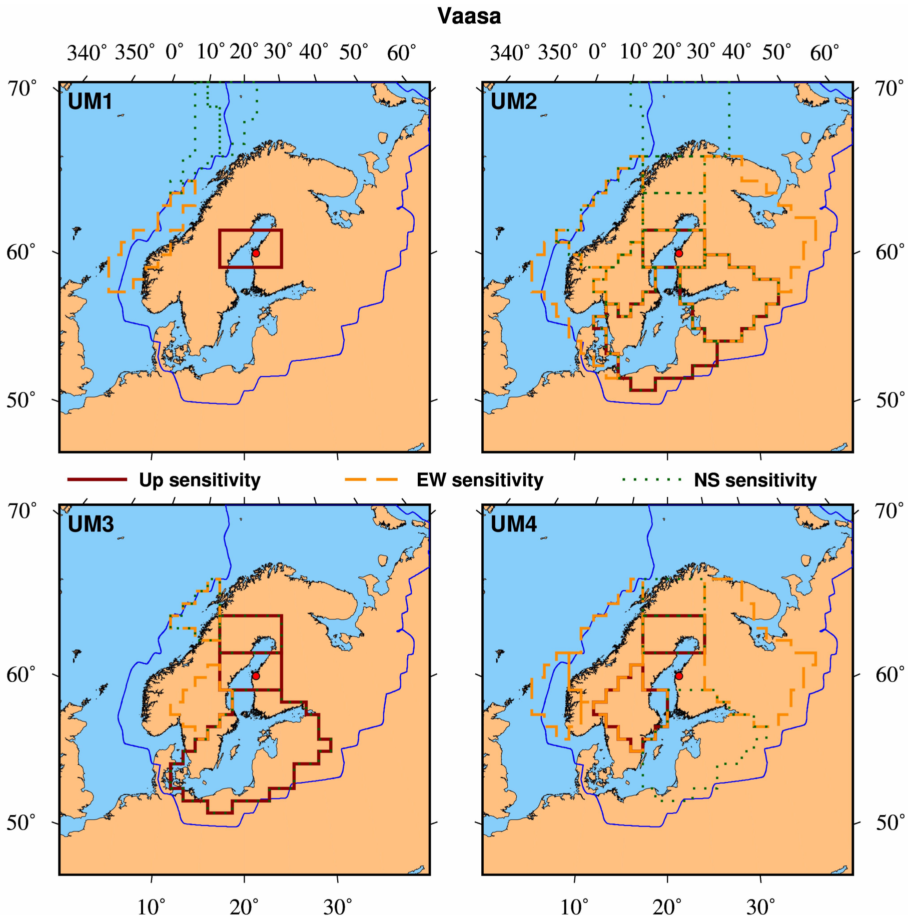

Fig. 6. Same as Fig. 4, but for Vaasa.

SED
5, 2389–2418, 2013

Sensitivity of GNSS stations to 3-D upper-mantle viscosity

H. Steffen and P. Wu

Title Page
Abstract
Introduction
Conclusions
References
Tables
Figures
◀▮ ▮▶
◀ ▶
Back
Close
Full Screen / Esc
Printer-friendly Version
Interactive Discussion

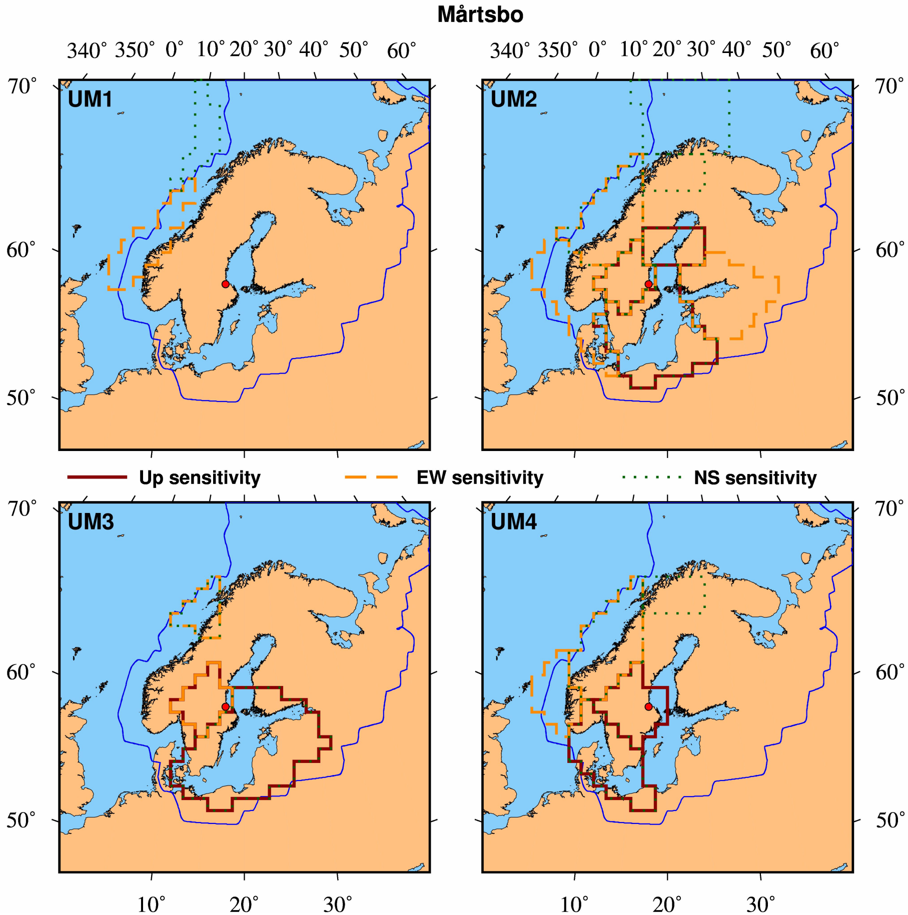

Fig. 7. Same as Fig. 4, but for Mårtsbo.

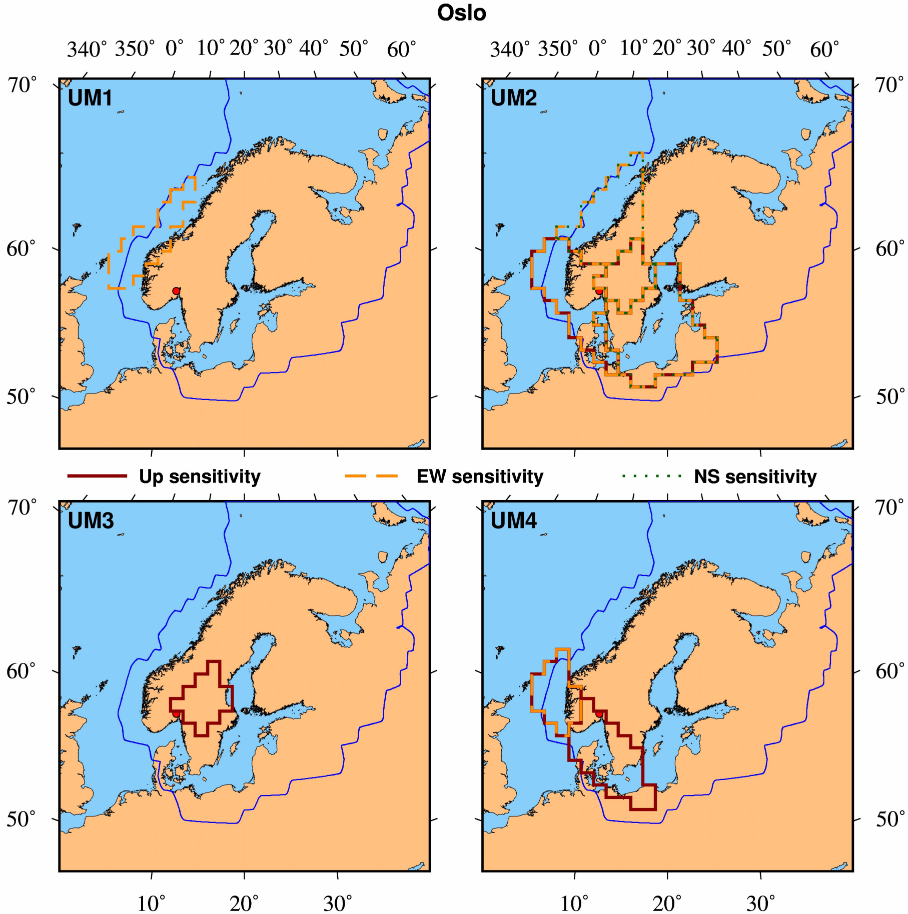

Fig. 8. Same as Fig. 4, but for Oslo.

SED
5, 2389–2418, 2013

Sensitivity of GNSS stations to 3-D upper-mantle viscosity

H. Steffen and P. Wu

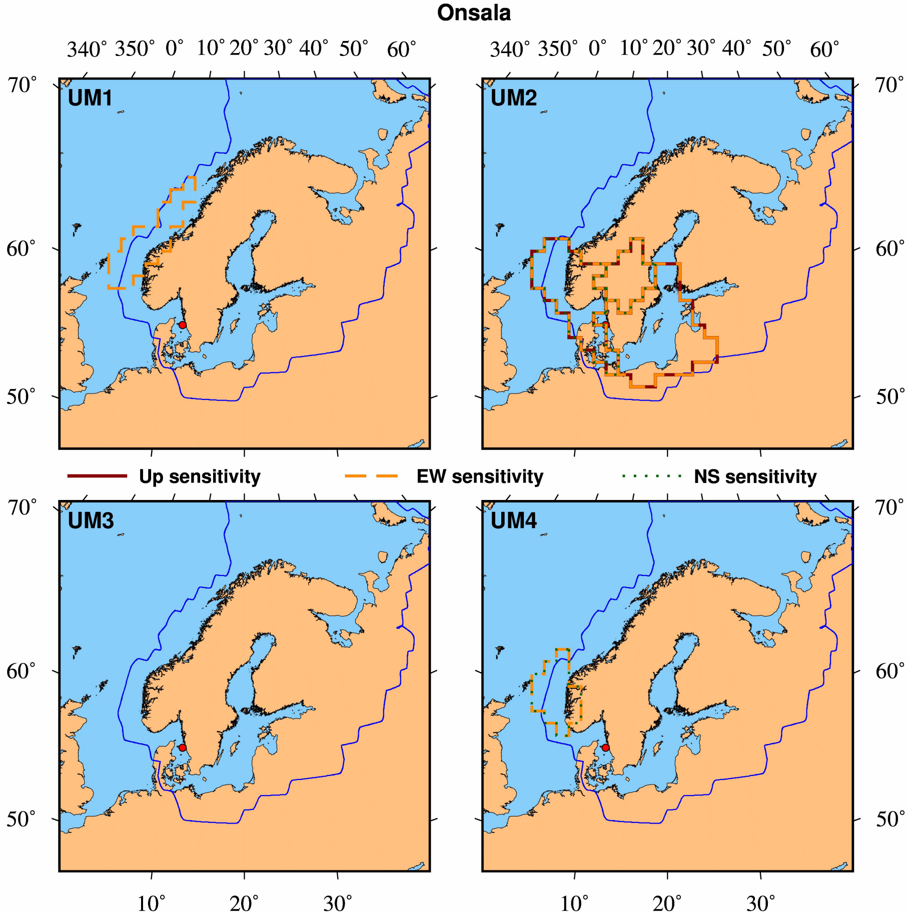

Fig. 9. Same as Fig. 4, but for Onsala.

SED
5, 2389–2418, 2013

Sensitivity of GNSS stations to 3-D upper-mantle viscosity

H. Steffen and P. Wu

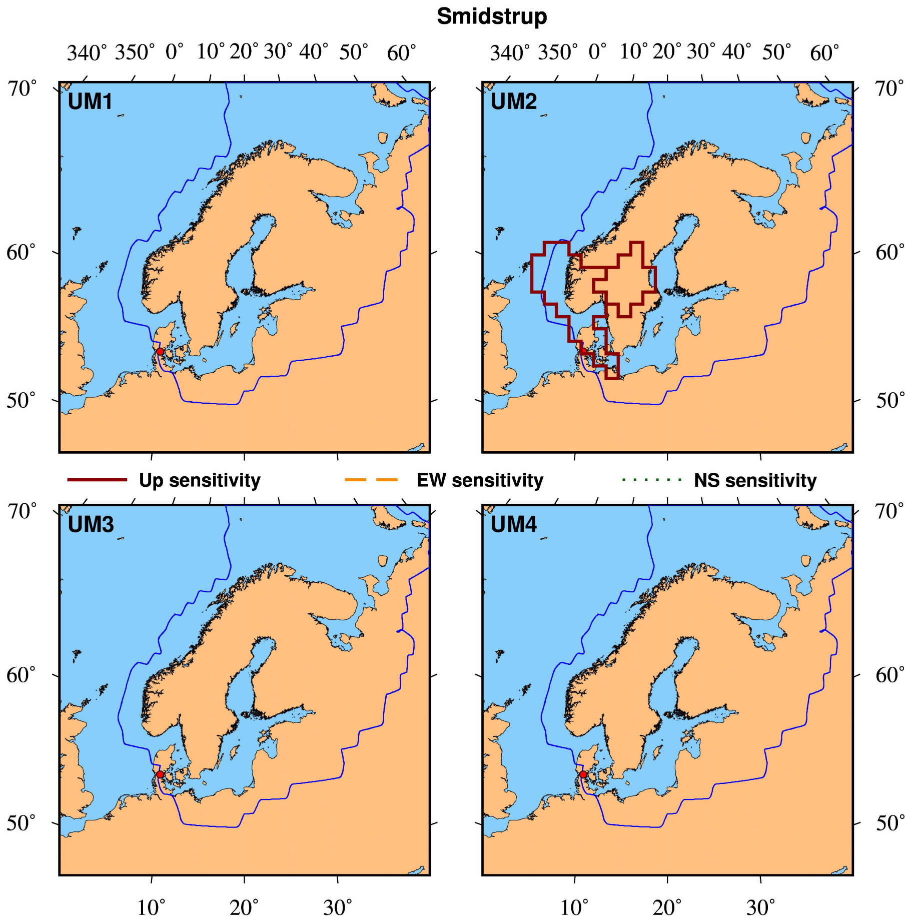

Fig. 10. Same as Fig. 4, but for Smidstrup.

SED

5, 2389–2418, 2013

Sensitivity of GNSS stations to 3-D upper-mantle viscosity

H. Steffen and P. Wu

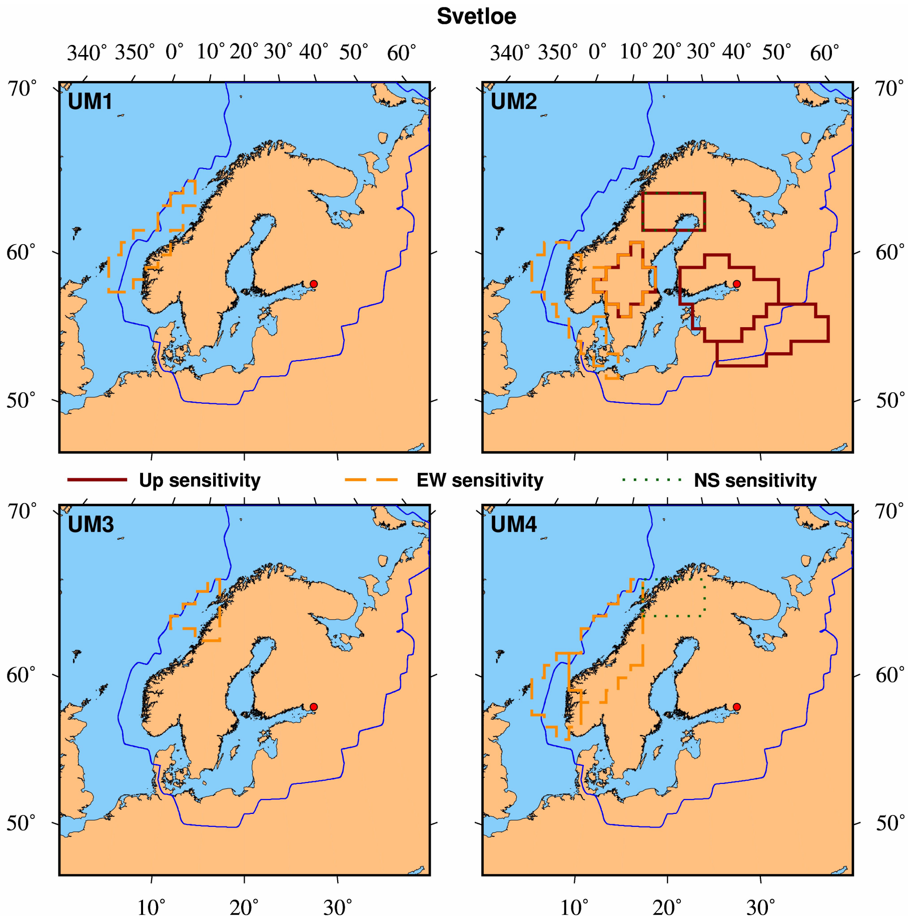

Fig. 11. Same as Fig. 4, but for Svetloe.

SED
5, 2389–2418, 2013

Sensitivity of GNSS stations to 3-D upper-mantle viscosity

H. Steffen and P. Wu

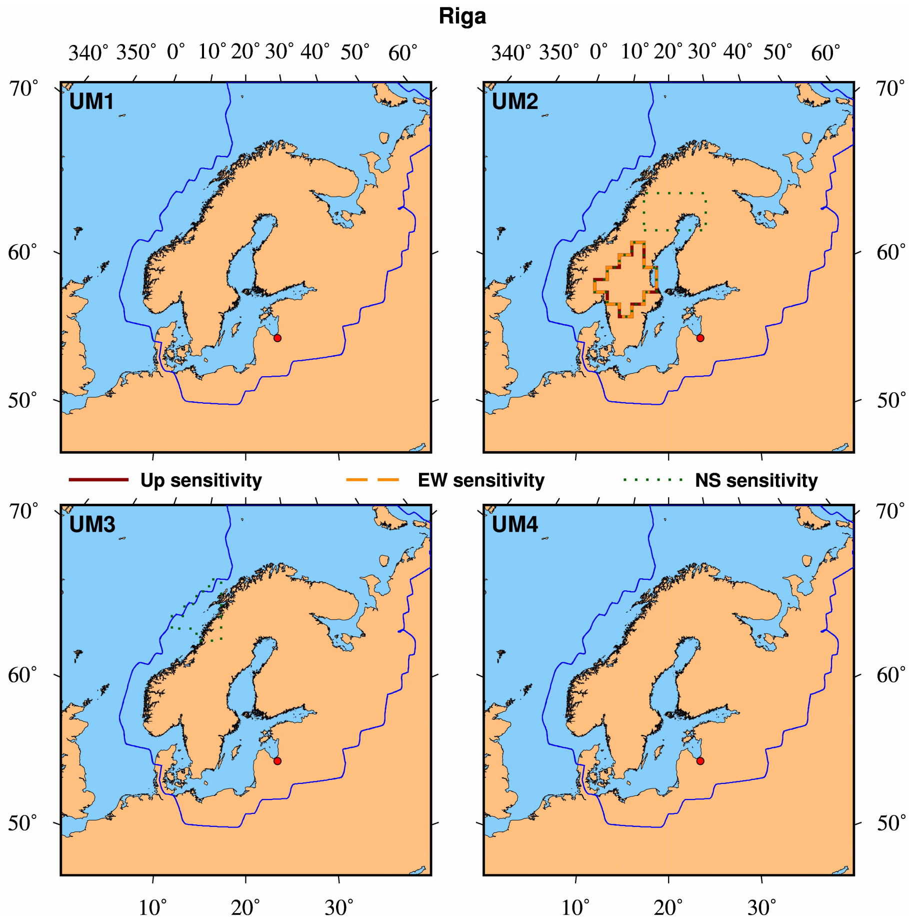

Fig. 12. Same as Fig. 4, but for Riga.

SED
5, 2389–2418, 2013

Sensitivity of GNSS stations to 3-D upper-mantle viscosity

H. Steffen and P. Wu